Curvature dependence of the electrolytic liquid-liquid interfacial tension

Markus Bier,[a] Joost de Graaf, Jos Zwanikken, and René van Roij
Institute for Theoretical Physics, Utrecht University, Leuvenlaan 4, 3584 CE Utrecht, The Netherlands

(Received 22 September 2008; accepted 2 December 2008; published online 12 January 2009)

The interfacial tension of a liquid droplet surrounded by another liquid in the presence of microscopic ions is studied as a function of the droplet radius. An analytical expression for the interfacial tension is obtained within a linear Poisson–Boltzmann theory and compared with numerical results from nonlinear Poisson–Boltzmann theory. The excess liquid-liquid interfacial tension with respect to the pure salt-free liquid-liquid interfacial tension is found to decompose into a curvature-independent part due to short-ranged interfacial effects and a curvature-dependent electrostatic contribution. Several curvature-dependent regimes of different scalings of the electrostatic excess interfacial tension are identified. Symmetry relations of the interfacial tension upon swapping droplet and bulk liquid are found to hold in the low-curvature limit, which, e.g., lead to a sign change of the excess Tolman length. For some systems a low-curvature expansion up to the second order turns out to be applicable if and only if the droplet size exceeds the Debye screening length in the droplet, independent of the Debye length in the bulk. © *2009 American Institute of Physics*. [DOI: 10.1063/1.3054372]

I. INTRODUCTION

Common wisdom in emulsion science tells that in order to kinetically stabilize an emulsion of water and oil, say, surfactants are needed in order to decrease the interfacial tension thereby decreasing the thermodynamic force causing droplet coalescence.[1] This picture has been upset by Leunissen *et al.*[2,3] who showed experimentally that, in certain additive-free water-oil mixtures, micron-sized water droplets in oil may be stabilized electrostatically by absorbing ions present in the system. Several aspects of these experiments such as the proposed charging of the water droplets due to an unequal partitioning[4–6] and the formation of a colloidal crystal of water droplets[7] can be understood theoretically within a simple Poisson–Boltzmann model. However, the rather unimodal size distribution of the water droplets in the above-mentioned experiments has not been explained so far. A similar observation has been made by Sacanna *et al.*[8] who found experimental indications of the existence of thermodynamically favored droplet radii in certain emulsions stabilized by nanosized colloids. A thermodynamically favored droplet radius requires a radius dependent water-oil interfacial tension because otherwise the global minimum of the free energy would be attained for one single macroscopic drop. One is thereby led to the problem of analyzing the liquid-liquid interfacial tension as a function of the droplet radius.

The study of the curvature dependence of liquid-vapor surface tensions has been pioneered by Gibbs,[9] Tolman,[10] and Kirkwood and Buff.[11] Tolman introduced a low-curvature expansion of the form $\gamma(a)/\gamma(\infty) \simeq 1/(1+2\delta/a) \simeq 1-2\delta/a$, where a denotes the radius of curvature, $\gamma(a)$ is the surface tension of the curved surface, and $\gamma(\infty)$ is its planar value. The parameter δ, which has the dimension of length, is called the *Tolman length* and it can be identified with the spatial distance between the Gibbs dividing surface and the surface of tension. In the past decades, the concept of a curvature dependent liquid-vapor surface tension has been taken up within various studies on critical phenomena,[12] interface elasticity,[13] and nucleation.[14,15]

However, whereas in all these investigations the droplet and the surrounding bulk were composed of the same substance, albeit in different phases, here a mixture of two different liquids and ions is studied. Moreover, only the excess interfacial tension due to the electrolyte is of interest here while the two liquids forming droplet and bulk merely act as external fields onto the ions.

The present investigation is carried out within the spherical version of the model studied in Ref. 5 (Sec. II). As in Ref. 5, linearization of the Poisson–Boltzmann equation offers the possibility of closed analytical expressions for the interfacial tension (Sec. III). In Sec. IV, the approximative analytical expressions for the interfacial tension will be shown to at least qualitatively, in many realistic cases even quantitatively, agree with the numerical results obtained within the full nonlinear theory. The main conclusion will be that it is precisely the electrostatic contribution to the interfacial tension that brings about a curvature dependence, which, however, is usually insignificant to serve as an explanation for unimodal radius distributions in the emulsions by Leunissen *et al.*[2,3] mentioned above (Sec. V). On the other hand, the curvature-dependent electrostatic contribution to the interfacial tension can be expected to increase considerably in magnitude if highly charged colloids instead of monovalent ions are present. Under these conditions, however, the approximations made in the present work are not *a priori* justified, and it is left for future studies to investigate the influence of valency on the qualitative picture to be drawn here, which corresponds to the low-valency limit.

[a]Electronic mail: m.bier@uu.nl.

II. MODEL AND FORMALISM

In the following, dimensionless quantities are expressed in units of the thermal energy k_BT, the elementary charge e, and the vacuum Bjerrum length $\ell = e^2/4\pi\varepsilon_{\text{vac}}k_BT$, with the permeability of the vacuum as ε_{vac}. Dimensionful quantities are denoted by the same symbol as the corresponding dimensionless quantities.

Consider a liquid spherical droplet of radius a and relative dielectric constant ε_d surrounded by bulk liquid of relative dielectric constant ε_b. Due to the spherical symmetry of the setting, the only relevant positional variable is the distance $r \in [0,\infty)$ from the droplet center. Monovalent cations (+ ions) and anions (− ions) are distributed in both liquids. The difference in solvation free energy of a $\pm$ ion in the droplet with respect to the bulk liquid is denoted by $f_\pm$, which, within the Born approximation,[16] can be estimated by $f_\pm = (1/2a_\pm)(1/\varepsilon_d - 1/\varepsilon_b)$ with the ion radius $a_\pm$. As derived in detail in Ref. 5, all interfacial effects due to, e.g., smooth interfaces, finite ion size, van der Waals forces, and image charges, which are short ranged as compared to the electrostatic potential, are accounted for by introducing solvent-induced ion potentials $V_\pm(r) = f_\pm\Theta(a+s-r)$ with Θ as the Heaviside function. Note that the parameter s, which describes the radial offset of the discontinuity of the solvent induced ion potentials $V_\pm$ with respect to the dielectric interface at $r=a$ and which is expected to be of the order of the size of a molecule or ion,[5] can be positive or negative, depending on whether the net effect of the abovementioned interfacial effects gives rise to a preference of the fluid structure in the droplet or in the bulk, respectively. More detailed representations of the interfacial effects are possible at the expense of more phenomenological parameters[17–19] but for the sake of convenience and because handy analytical expressions are desired, the present most simple choice is made here.

A convenient approach to calculate the interfacial tension of the system under consideration is to first determine the equilibrium ion number density profiles $\varrho_\pm$ by means of the density functional theory[20–22] and then to infer the interfacial tension from inserting these equilibrium profiles into the grand potential density functional. The Poisson–Boltzmann theory corresponds to the mean-field grand potential density functional

$$\Omega[\varrho_\pm] = 4\pi\sum_{\alpha=\pm}\int_0^\infty dr\ r^2\varrho_\alpha(r) \times\left(\ln(\varrho_\alpha(r)) - 1 - \mu_\alpha + V_\alpha(r) + \frac{\alpha}{2}\phi(r,[\varrho_\pm])\right), \tag{1}$$

with μ_α as the chemical potential of α ions and $\phi(r,[\varrho_\pm])$ as the electrostatic potential functional at radius r, which fulfills the Poisson equation

$$\frac{1}{r^2}(\varepsilon(r)r^2\phi'(r,[\varrho_\pm]))' = -4\pi\sum_{\alpha=\pm}\alpha\varrho_\alpha(r), \tag{2}$$

subject to the boundary conditions $\phi'(r=0)=0$ and $\phi(r=\infty)=0$, where a prime denotes a derivative with respect to r and $\varepsilon(r) := \varepsilon_d\Theta(a-r) + \varepsilon_b\Theta(r-a)$. The electrostatic potential is a continuous function of r and, at the dielectric interface $(r=a)$, the radial component of the dielectric displacement is continuous, $\varepsilon_d\phi'(r\nearrow a) = \varepsilon_b\phi'(r\searrow a)$.

Minimizing the density functional in Eq. (1) gives rise to the Euler–Lagrange equations,

$$\varrho_\alpha(r) = \exp(\mu_\alpha - V_\alpha(r) - \alpha\phi(r,[\varrho_\pm])). \tag{3}$$

Due to the local charge neutrality in the bulk liquid far away from the droplet $(\varrho_+(r=\infty) = \varrho_-(r=\infty))$, one infers $\mu_+ = \mu_- =: \mu$. Upon introducing the reference densities $\varrho_b^{\text{ref}} := \exp(\mu)$ and $\varrho_d^{\text{ref}} := \varrho_b^{\text{ref}}\exp(-(f_+ + f_-)/2)$, the sharp-kink reference density profile $\varrho^{\text{ref}}(r,x) := \varrho_b^{\text{ref}}\Theta(r-x) + \varrho_d^{\text{ref}}\Theta(x-r)$ with the discontinuity located at radius x, and the shifted electrostatic potential $\psi(r) := \phi(r) - \phi_D\Theta(a+s-r)$ with the Donnan potential $\phi_D := (f_- - f_+)/2$, the Euler–Lagrange equation [Eq. (3)] can be rewritten as

$$\varrho_\alpha(r) = \varrho^{\text{ref}}(r,a+s)\exp(-\alpha\psi(r)). \tag{4}$$

Inserting Eq. (4) into the Poisson equation [Eq. (2)] leads to the Poisson–Boltzmann equation,

$$\psi''(r) = \kappa(r)^2\sinh(\psi(r)), \quad r \neq a, a+s, \tag{5}$$

with $\kappa(r) := \sqrt{8\pi\varrho^{\text{ref}}(r,a+s)/\varepsilon(r)}$ as the Debye screening factor. Given a solution ψ, the interfacial tension with respect to the dielectric interface at $r=a$ in excess to the pure salt-free liquid-liquid interfacial tension between the droplet and the bulk liquid is, after inserting Eq. (4) into Eq. (1), determined by

$$\gamma^{\text{ex}} = \frac{\Omega[\varrho_\pm] - \Omega[\varrho^{\text{ref}}(\cdot,a)]}{4\pi a^2} = -\frac{1}{a^2}\sum_{\alpha=\pm}\int_0^\infty dr\ r^2\left(\varrho_\alpha(r) - \varrho^{\text{ref}}(r,a) + \frac{\alpha}{2}\varrho_\alpha(r)\phi(r,[\varrho_\pm])\right). \tag{6}$$

As solutions of the nonlinear Poisson–Boltzmann [Eq. (5)] in the spherical geometry can be obtained only numerically, the same holds for the excess interfacial tension γ^{ex} in Eq. (6). However, upon linearizing the Euler–Lagrange equation [Eq. (4)] and the Poisson–Boltzmann equation [Eq. (5)] one obtains analytical expressions for the excess interfacial tension γ^{ex}, which will be derived in the next section.

III. LINEARIZED THEORY

For a sufficiently small Donnan potential $|\phi_D| < 1$, the Euler–Lagrange equation [Eq. (4)] and the Poisson–Boltzmann equation [Eq. (5)] can be linearized, leading to

$$\varrho_\alpha(r) = \varrho^{\text{ref}}(r,a+s)(1 - \alpha\psi(r)) \tag{7}$$

and

$$\psi''(r) = \kappa(r)^2\psi(r), \quad r \neq a, a+s, \tag{8}$$

respectively. Inserting both expressions into Eq. (6), one obtains

$$\gamma^{\mathrm{ex}} = 2s(\varrho_b^{\mathrm{ref}} - \varrho_d^{\mathrm{ref}})\left(1 + \frac{s}{a} + \frac{1}{3}\left(\frac{s}{a}\right)^2\right) - \frac{\phi_D}{2}\left(1 + \frac{s}{a}\right)^2 \sigma(a+s), \tag{9}$$

with

$$\sigma(r) := -\frac{\varepsilon(r)\psi'(r)}{4\pi} \tag{10}$$

as the charge enclosed by a sphere of radius r around the origin per sphere surface area.

The linear Poisson–Boltzmann equation [Eq. (8)] is analytically soluble, which gives rise to an expression of the form

$$\sigma(a+s) = \frac{\phi_D}{\left(1 + \frac{s}{a}\right)^2}\sqrt{\frac{\varepsilon_b \varrho_b^{\mathrm{ref}}}{2\pi}} F(s/a, \kappa_b a, n, p), \tag{11}$$

where $\kappa_b := \sqrt{8\pi\varrho_b^{\mathrm{ref}}/\varepsilon_b}$, $n := \sqrt{\varepsilon_d/\varepsilon_b}$, and $p := \sqrt{\varrho_d^{\mathrm{ref}}/\varrho_b^{\mathrm{ref}}}$. The full scaling function F, which is recorded in the Appendix, appears somewhat lengthy but is straightforward to obtain in principle.

However, since the effective interfacial width parameter s is usually very much smaller than the droplet radius and the local Debye lengths, $|s| \ll a, \kappa(r)^{-1}$, the first argument of the scaling function F can, within an excellent approximation, be set to zero. Inserting $x=0$ into Eqs. (A1) and (A2) leads to

$$F(0,y,n,p) = \frac{np + \frac{n(p-n)}{y} - \left(\frac{n}{y}\right)^2 + \exp\left(-2y\frac{p}{n}\right)\left(np + \frac{n(p+n)}{y} + \left(\frac{n}{y}\right)^2\right)}{1 + np + \frac{1-n^2}{y} + \exp\left(-2y\frac{p}{n}\right)\left(-1 + np - \frac{1-n^2}{y}\right)}. \tag{12}$$

At this level of approximation Eqs. (9) and (11) reduce to

$$\gamma^{\mathrm{ex}} = 2s\varrho_b^{\mathrm{ref}}(1-p^2) - \frac{\phi_D}{2}\sigma(a) \tag{13}$$

and

$$\sigma(a) = \phi_D\sqrt{\frac{\varepsilon_b\varrho_b^{\mathrm{ref}}}{2\pi}} F(0, \kappa_b a, n, p), \tag{14}$$

respectively. According to Eq. (14), the droplet charge per droplet surface area $\sigma(a)$ is (almost) independent of the interfacial width s. On the other hand, the excess interfacial tension γ^{ex} in Eq. (13) comprises a contribution describing the ion exclusion due to the short-ranged *interfacial effects*,

$$\gamma_{\mathrm{ie}}^{\mathrm{ex}} := 2s\varrho_b^{\mathrm{ref}}(1-p^2), \tag{15}$$

which is (essentially) linear in s and (almost) independent of the droplet radius a, as well as an *electrostatic* contribution,

$$\gamma_{\mathrm{es}}^{\mathrm{ex}} := -\frac{\phi_D}{2}\sigma(a), \tag{16}$$

which is (almost) independent of the effective interfacial width s.

In order to understand the involved dependence of the scaling function $F(0,y,n,p)$ on y it is useful to investigate the asymptotic behavior for large and small values of y. If $y \gg y_1^\times := n/p$, the terms in Eq. (12) proportional to the exponentials may be neglected such that

$$F(0, y \gg y_1^\times, n, p) \simeq \frac{np}{1+np} G(y,n,p), \tag{17}$$

with

$$G(y,n,p) := \frac{\left(1 - \frac{n}{py}\right)\left(1 + \frac{1}{y}\right)}{1 + \frac{1-n^2}{(1+np)y}}. \tag{18}$$

Defining $y_2^\times := (|1-n^2|)/(1+np)$ and $y_3^\times := 1$ and noting that $(1-n^2)/(1+np) \in [-y_1^\times, y_3^\times]$, one infers from Eq. (17) the leading order asymptotic behavior,

$$F(0, y \gg y_1^\times, n, p) \simeq \begin{cases} \dfrac{np}{1+np}, & (\mathrm{I}) y \gg y_3^\times \\ \dfrac{np}{1+np} y^{-1}, & (\mathrm{II}) y_2^\times \ll y \ll y_3^\times \\ \dfrac{np}{1-n^2}, & (\mathrm{III}) y \ll y_2^\times. \end{cases} \tag{19}$$

The three cases considered in Eq. (19) are exhaustive and mutually exclusive for $y \gg y_1^\times$ because $y_2^\times \leq \max(y_1^\times, y_3^\times)$. If $y \ll y_1^\times$, Eq. (12) leads to

$$F(0, y \ll y_1^\times, n, p) \simeq \frac{p^2}{3} y. \tag{20}$$

Figure 1 displays $F(0,y,n,p)$ for the case $y_1^\times \ll y_2^\times \ll y_3^\times$, where all four asymptotic regimes I–IV of Eqs. (19) and (20) are apparent. If $y_2^\times \ll y_1^\times \ll y_3^\times$, however, regime III in Fig. 1 is absent, and a crossover between regimes II and IV takes place at $y = y_1^\times$. Moreover, if $y_1^\times \gg y_3^\times$, regime II is also absent, and $F(0,y,n,p)$ exhibits a single crossover at $y = y_1^\times$ between regimes I and IV.

According to $y = \kappa_b a$ [see Eqs. (11) and (14)] the crossover values $y_i^\times, i \in \{1,2,3\}$ correspond to crossover droplet

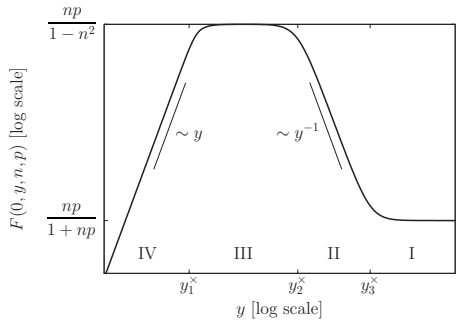

FIG. 1. Scaling function $F(0,y,n,p)$ as a function of y for the relation $y_1^\times \ll y_2^\times \ll y_3^\times$ of the crossover positions (see main text) in a log-log plot. The asymptotic regimes I–IV corresponding to Eqs. (19) and (20) are apparent. For $y_1^\times \gg y_2^\times$, regime III is absent, and for $y_1^\times \gg y_3^\times$ regime II is also absent.

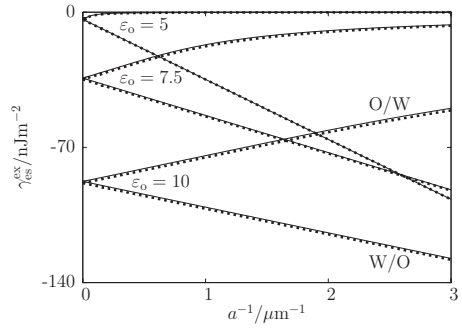

FIG. 2. Electrostatic contribution to the excess interfacial tension $\gamma_{\rm es}^{\rm ex}$ in mixtures of oil ($\varepsilon_o \in \{5,7.5,10\}$) and water ($\varepsilon_w=80$) as a function of the radius a of an oil droplet in water (O/W, ascending curves) and a water droplet in oil (W/O, descending curves) with ion radii $a_+=0.36$ nm and $a_-=0.30$ nm, as well as an ionic strength in water $I_w=1$ mM. The thin solid curves are calculated by means of the analytical expressions within the linear theory of Sec. III, whereas the thick dotted curves are obtained by numerically solving the nonlinear Poisson–Boltzmann equation [Eq. (5)]. Upon swapping oil and water ($\mathrm{O/W} \leftrightarrow \mathrm{W/O}$) the slope of the curves at $a^{-1}=0$ (planar system) changes its sign.

radii $a_i^\times, i \in \{1,2,3\}$, i.e., regimes I–IV can be understood in terms of length scales of the system. Obviously $a_3^\times = \kappa_b^{-1}$ and $a_1^\times = \kappa_d^{-1} := \kappa_b^{-1} n/p$ equal the Debye lengths in the bulk and in the droplet, respectively. Finally $a_2^\times = |\varepsilon_b - \varepsilon_d|/(\varepsilon_b \kappa_b + \varepsilon_d \kappa_d)$ is a length scale that accounts for the dielectric contrast between bulk and droplet.

It will turn out in the next section that the analytical expressions based on the linearized theory derived in the present section agree qualitatively, in typical cases even quantitatively, with numerically calculated interfacial tensions within the nonlinear theory.

IV. DISCUSSION

Here the closed analytical expressions obtained within the linearized Poisson–Boltzmann theory of the previous section are discussed and compared with numerical results obtained within the nonlinear theory based on Eqs. (4)–(6). Some of the numerical data presented here have already been considered in Ref. 7. Throughout this section, one of the liquids is water with a dielectric constant of $\varepsilon_w=80$. Moreover, the largely arbitrary but representative choice of ion radii $a_+=0.36$ nm and $a_-=0.30$ nm is made throughout. Given the dielectric constant of the second liquid, called "oil," the parameters n, p, and ϕ_D are known within the Born approximation (see Sec. II). The cases of an oil droplet in water (O/W) and of a water droplet in oil (W/O) will be distinguished.

Figure 2 displays the electrostatic contribution to the excess interfacial tension $\gamma_{\rm es}^{\rm ex}$ [see Eq. (16)] of oil droplets in water (O/W, ascending curves) and water droplets in oil (W/O, descending curves) for an ionic strength in water $I_w=1$ mM, where $I_w := \varrho_b^{\rm ref}$ for O/W and $I_w := \varrho_d^{\rm ref}$ for W/O, as a function of the droplet radius a. The analytical expression Eq. (16) within the linearized Poisson–Boltzmann theory (thin solid curves) is compared with numerical results of the nonlinear Poisson–Boltzmann theory (thick dotted curves). The slight quantitative differences are due to the linearization approximation and they are already present in the planar system ($a^{-1}=0$). The quantities n, p, and ϕ_D, as well as the crossover values $y_1^\times$ and $y_2^\times$ corresponding to the curves in Fig. 2, are displayed in Table I. According to Sec. III, regime III is expected to be absent for the W/O systems because $y_3^\times > y_1^\times > y_2^\times$, whereas regimes II and III are absent for the O/W systems because $y_1^\times > y_3^\times > y_2^\times$ (see also the discussion of Fig. 5 at the end of this section).

Due to Eq. (16) the relative change in the electrostatic excess interfacial tension $\gamma_{\rm es}^{\rm ex}(a)$ and the droplet charge per droplet surface area $\sigma(a)$ with respect to their planar values $\gamma_{\rm es}^{\rm ex}(\infty)$ and $\sigma(\infty)$, respectively, are equal, and they exhibit the low-curvature asymptotic behavior [see Eqs. (14) and (17)],

$$\frac{\gamma_{\rm es}^{\rm ex}(a)}{\gamma_{\rm es}^{\rm ex}(\infty)} = \frac{\sigma(a)}{\sigma(\infty)} \simeq G(\kappa_b a,n,p), \quad \kappa_b a \gg y_1^\times, \tag{21}$$

where G is as defined in Eq. (18). Upon rewriting Eq. (18) one recognizes the asymptotic behavior,

$$G(y \gg y_2^\times,n,p) = 1 - \frac{n(1-p^2)}{p(1+np)} y^{-1} - \frac{\dfrac{n(p+n)^2}{p(1+np)^2} y^{-2}}{1+\mathrm{sign}(1-n)\dfrac{y_2^\times}{y}}$$

$$\simeq 1 - \frac{n(1-p^2)}{p(1+np)} y^{-1} - \frac{n(p+n)^2}{p(1+np)^2} y^{-2}, \tag{22}$$

which equals the expansion in y^{-1} up to the second order. Hence, the low-curvature expansion up to the second order in a^{-1} obtained by combining Eqs. (21) and (22) is expected to be accurate if $\kappa_b a \gg y_1^\times, y_2^\times$. Traditionally, empirically motivated expansions in a^{-1} have been used to represent the curvature dependence of the interfacial tension without knowing their applicability *a priori*. However, it has been argued by König *et al.*,[23] on the basis of a morphometrical approach, that the deviation of intensive thermodynamic quantities from their planar values are linear combinations of the mean and the Gaussian curvature *provided* the geometrical length scales are much larger than any correlation length, i.e., $a \gg \kappa_d^{-1}, \kappa_b^{-1}$ or equivalently $\kappa_b a \gg y_1^\times, y_3^\times$. This condition is only sufficient but not necessary for the validity of the above low-curvature expansion because it already implies $\kappa_b a \gg y_2^\times$ due to $y_2^\times \le \max(y_1^\times, y_3^\times)$. For $n,p \gg 1$, the low-curvature expansion is valid if $\kappa_d a \gg 1$, *independent* of the

TABLE I. Quantities n, p, and ϕ_D, as well as the crossover values $y_1^\times$ and $y_2^\times$ (see Secs. II and III), within the Born approximation for (a) O/W and (b) W/O systems with the oil dielectric constant $\varepsilon_o \in \{5, 7.5, 10\}$ and ion radii $a_+ = 0.36$ nm and $a_- = 0.30$ nm.

O/W					
ε_o	n	p	ϕ_D	$y_1^\times$	$y_2^\times$
5	0.25	0.000 285	1.48	876	0.937
7.5	0.306	0.005 20	0.956	58.9	0.905
10	0.354	0.0222	0.692	15.9	0.868
W/O					
ε_o	n	p	ϕ_D	$y_1^\times$	$y_2^\times$
5	4	3500	−1.48	0.001 14	0.001 07
7.5	3.27	192	−0.956	0.0170	0.0154
10	2.83	45.1	−0.692	0.0627	0.0545

bulk Debye length κ_b^{-1}, because in this case $y_2^\times \approx y_1^\times$. This is the case, e.g., for the W/O systems considered in Table I.

From Eq. (18) one straightforwardly recognizes the symmetry $G(py/n, 1/n, 1/p) = G(-y, n, p)$, which means that swapping droplet and bulk liquid, i.e., $p \mapsto 1/p$, $n \mapsto 1/n$, and $\kappa_b \mapsto \kappa_d$, while keeping the droplet radius a fixed has numerically the same effect on function G as inverting the sign of the droplet radius. Due to this symmetry one concludes for the coefficients of an expansion in inverse powers of a, as in Eq. (22) for $y = \kappa_b a$, that, upon swapping droplet and bulk liquid, the odd-order coefficients merely invert their sign, whereas the even-order coefficients do not change. This phenomenon can be observed in Fig. 2, where the slope close to the planar limit ($a^{-1} = 0$), which is proportional to the excess Tolman length due to the presence of ions, simply changes its sign upon swapping oil and water (O/W $\leftrightarrow$ W/O).

Figure 3 exhibits the electrostatic contribution to the excess interfacial tension $\gamma_{\mathrm{es}}^{\mathrm{ex}}$ as a function of the dielectric constant ε_o of the oil for the ionic strength in water $I_w = 1$ mM and for various droplet radii $a \in \{50, 100, 250, 500, 1000\ \mathrm{nm}, \infty\}$. As in Fig. 2, the thin solid curves correspond to the analytic linear theory of Sec. III, whereas the thick dotted curves are the numerical results of the nonlinear scheme. Quantitative agreement is observed, even in the low-ε_o range where the Donnan potential ϕ_D is *not* small and the linearization approximation is *not a priori* justified. From the linearized theory of Sec. III, one can derive the asymptotic behavior $\gamma_{\mathrm{es}}^{\mathrm{ex}} = \mathcal{O}(-(\varepsilon_o - \varepsilon_w)^2)$ for $\varepsilon_o \to \varepsilon_w$ as well as $\gamma_{\mathrm{es}}^{\mathrm{ex}} = \mathcal{O}(-\exp(-\mathrm{const}/\varepsilon_o))$ for an O/W system and $\gamma_{\mathrm{es}}^{\mathrm{ex}} = \mathcal{O}(-1/\varepsilon_o)$ for a W/O system as $\varepsilon_o \to 0$. This behavior is apparent in Fig. 3, too.

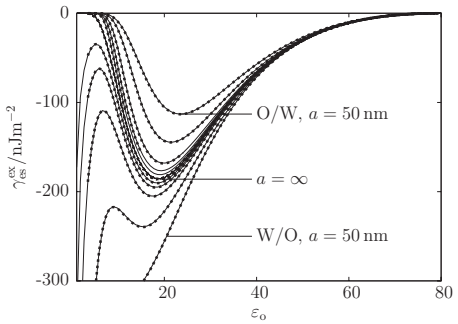

FIG. 3. Electrostatic contribution to the excess interfacial tension in mixtures of oil and water ($\varepsilon_w = 80$) as a function of the dielectric constant ε_o of the oil for droplet radii $a \in \{50, 100, 250, 500, 1000\ \mathrm{nm}, \infty\}$ of an oil droplet in water (O/W) and a water droplet in oil (W/O) with ion radii $a_+ = 0.36$ nm and $a_- = 0.30$ nm as well as the ionic strength in water $I_w = 1$ mM. The thin solid curves are calculated by means of the analytical expressions within the linear theory of Sec. III, whereas the thick dotted curves are obtained by numerically solving the nonlinear Poisson–Boltzmann equation [Eq. (5)]. There is quantitative agreement between the linear and the nonlinear theory for the ranges of a and ε_o considered here.

The total excess interfacial tension γ^{ex} comprises not only the electrostatic part $\gamma_{\mathrm{es}}^{\mathrm{ex}}$ but also the contribution $\gamma_{\mathrm{ie}}^{\mathrm{ex}}$ due to the interfacial effects [see Eq. (15)]. It is readily seen that $\gamma_{\mathrm{ie}}^{\mathrm{ex}} = \pm\mathcal{O}(s(\varepsilon_w - \varepsilon_o))$ for $\varepsilon_o \to \varepsilon_w$ and $\gamma_{\mathrm{ie}}^{\mathrm{ex}} = \pm\mathcal{O}(s)$ for $\varepsilon_o \to 0$, where the upper (+) and the lower (−) signs correspond to an O/W and a W/O system, respectively. Hence, if $s \neq 0$, the interfacial effects will dominate over the electrostatic effects in the limits $\varepsilon_o \to 0$ for O/W systems and $\varepsilon_o \to \varepsilon_w$ for arbitrary systems. Figure 4 displays the total excess interfacial tension corresponding to the parameters used in Fig. 3 and an interfacial width parameter s with $|s| = 0.33$ nm on the water side of the interface, i.e., $s > 0$ for O/W and $s < 0$ for W/O.

According to the results of Sec. III, the electrostatic ex-

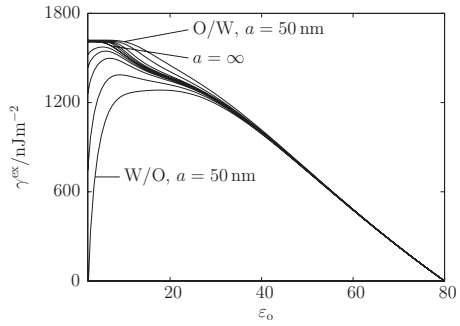

FIG. 4. Total excess interfacial tension in mixtures of oil and water ($\varepsilon_w = 80$) as a function of the dielectric constant ε_o of the oil for droplet radii $a \in \{50, 100, 250, 500, 1000\ \mathrm{nm}, \infty\}$ of an oil droplet in water (O/W) and a water droplet in oil (W/O), with ion radii $a_+ = 0.36$ nm and $a_- = 0.30$ nm, interfacial width parameter $|s| = 0.33$ nm, as well as the ionic strength in water $I_w = 1$ mM.

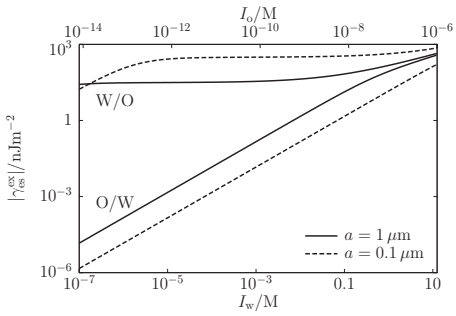

FIG. 5. Electrostatic excess interfacial tension in mixtures of oil (ε_o=5) and water (ε_w=80) as a function of the ionic strength in oil (I_o) or water (I_w) for droplet radii $a \in \{0.1, 1\ \mu\text{m}\}$ of an oil droplet in water (O/W) and a water droplet in oil (W/O) with ion radii a_+=0.36 nm and a_-=0.30 nm. The O/W system exhibits only regimes I and IV (see main text and Fig. 1), whereas for the W/O system, regimes I, II, and IV are present. Upon changing the droplet size a, the crossover ionic strengths shift by a factor of a^{-2}.

cess interfacial tension γ_{es}^{ex} as a function of the bulk ionic strength $I_b := \varrho_b^{ref}$ can be asymptotically described by

$$\gamma_{es}^{ex} \simeq \begin{cases} -\phi_D^2 \sqrt{\dfrac{\varepsilon_b}{8\pi}} \dfrac{np}{1+np} I_b^{1/2}, & \text{(I)} I_b \gg I_{b1}^{\times}, I_{b3}^{\times} \\ -\phi_D^2 \dfrac{\varepsilon_b}{8\pi} \dfrac{np}{(1+np)a}, & \text{(II)} I_{b1}^{\times}, I_{b2}^{\times} \ll I_b \ll I_{b3}^{\times} \\ -\phi_D^2 \sqrt{\dfrac{\varepsilon_b}{8\pi}} \dfrac{np}{1-n^2} I_b^{1/2}, & \text{(III)} I_{b1}^{\times} \ll I_b \ll I_{b2}^{\times} \\ -\phi_D^2 \dfrac{p^2}{3} a I_b, & \text{(IV)} I_b \ll I_{b1}^{\times}, \end{cases} \tag{23}$$

with the crossover bulk ionic strengths $I_{bk}^{\times} := \varepsilon_b (y_k^{\times})^2 / 8\pi a^2$, $k \in \{1,2,3\}$ where the $y_k^{\times}, k \in \{1,2,3\}$ are defined in Sec. III. For a planar system ($a=\infty$) the crossovers are at zero ionic strength, hence only the high-ionic strength regime I in Fig. 1 ($I_b \gg I_{b1}^{\times}, I_{b3}^{\times}$) is present, which coincides exactly with the electrostatic contribution to the excess interfacial tension in Ref. 5.

For an oil dielectric constant ε_o=5 and a droplet radius a=1 μm the crossover bulk ionic strengths are $I_{b1}^{\times} \approx 71$ mM, $I_{b2}^{\times} \approx 82$ nM, $I_{b3}^{\times} \approx 93$ nM for an O/W system, where $I_b = I_w$ is the ionic strength in water, and $I_{b1}^{\times} \approx 7.6$ fM, $I_{b2}^{\times} \approx 6.6$ fM, $I_{b3}^{\times} \approx 5.8$ nM for a W/O system, where $I_b = I_o$ is the ionic strength in oil (see Table I). Here, ionic strengths in oil I_o and in water I_w are related to each other by $I_o / I_w \approx 8.1 \times 10^{-8}$. Figure 5 displays γ_{es}^{ex} as a function of the ionic strength in the physical range $I_w \in [10^{-7} M, 10M]$ for the droplet radii a=1 μm and a=0.1 μm. The crossover ionic strengths of the latter droplet size are larger by a factor of 100 as compared to the former because $I_{bk}^{\times} \sim a^{-2}$. By inspection of the values of the crossover bulk ionic strengths, one expects only regimes I and IV of Fig. 1 to be present for the O/W system, whereas regimes I, II, and IV are expected for the W/O system. The occurrence of regimes I and IV for the O/W system and I, II, and IV for the W/O system can be inferred from Fig. 5 in conjunction with Eq. (23).

V. CONCLUSIONS AND SUMMARY

It turned out in the previous section that the analytical theory of Sec. III based on a linearized Poisson–Boltzmann theory is in good (at least) qualitative agreement with the results from the full nonlinear theory. It can therefore be expected that the general conclusions drawn from that linear theory apply to more elaborate models[17–19] too.

According to Eqs. (13), (15), and (16), the excess liquid-liquid interfacial tension is $\gamma^{ex} = \gamma_{ie}^{ex} + \gamma_{es}^{ex}$, where the curvature dependence is essentially only due to the electrostatic part γ_{es}^{ex}, and not due to the contribution of the short-ranged interfacial effects γ_{ie}^{ex}. While γ^{ex} can indeed be negative, thereby decreasing the total interfacial tension, the largest magnitude $|\gamma^{ex}|$ is attained at high ionic strengths where $\gamma^{ex} \approx \gamma_{ie}^{ex}$, i.e., where γ^{ex} is essentially curvature independent. One has to conclude that the unimodal droplet size distribution of W/O emulsions observed by Leunissen *et al.*[2,3] *cannot* be explained by the curvature dependence of the interfacial tension due to electrostatic effects alone. However, this conclusion does not apply to the experiments by Sacanna *et al.*,[8] where highly charged colloids instead of monovalent ions are present, as the linearized theory of Sec. III is not *a priori* justified for multivalent ions or highly charged colloids. Instead it is an interesting open question to be addressed in future studies as to what extent the qualitative low-valency picture drawn here is valid for the presence of high-valency particles.

In summary, the curvature dependence of the electrolytic liquid-liquid interfacial tension within a simple linear Poisson–Boltzmann model in the spherical geometry has been calculated analytically. This linear theory turned out to be at least qualitatively reliable as has been checked by numerically solving the corresponding nonlinear Poisson–Boltzmann model. Novel low ionic strength regimes, which are not present for a planar liquid-liquid interface, have been identified. Low and high curvature asymptotics of the interfacial tension have been discussed. In particular, it has been found that in systems where the ionic strength and the dielectric constant in the droplet are much larger than in the bulk the range of validity of low-curvature expansions up to the second order in the inverse radius of curvature is independent of the bulk Debye length.

ACKNOWLEDGMENTS

This work is part of the research program of the "Stichting voor Fundamenteel Onderzoek der Materie" (FOM), which is financially supported by the "Nederlandse Organisatie voor Wetenschappelijk Onderzoek" (NWO).

APPENDIX: SCALING FUNCTION *F*

Upon solving the linearized Poisson–Boltzmann equation [Eq. (8)] one obtains analytical solutions for the shifted electrostatic potential ψ, which, via Eq. (10), determines the scaling function F introduced in Eq. (11),

$$F(x,y,n,p) = \begin{cases} \dfrac{T_1\left(p(1+x) - \dfrac{n}{y} + \exp\left(-2y\dfrac{p}{n}(1+x)\right)\left(p(1+x) + \dfrac{n}{y}\right)\right)}{T_2 + \exp\left(-2y\dfrac{p}{n}(1+x)\right)T_3}, & x < 0 \\ p\left(1 + x + \dfrac{1}{y}\right)\dfrac{T_4 + \exp\left(-2y\dfrac{p}{n}\right)T_5}{T_6 + \exp\left(-2y\dfrac{p}{n}\right)T_7}, & x > 0, \end{cases} \tag{A1}$$

where

$$T_1 := n\left(1 + x + \frac{1}{y} + \frac{(1-n^2)x}{y}\right)\cosh\left(\frac{xy}{n}\right) - n^2\left(1 + x + \frac{1}{y} + \frac{1-n^2}{y^2}\right)\sinh\left(\frac{xy}{n}\right),$$

$$T_2 := \left(1 + np + \frac{1-n^2}{y}\right)\cosh\left(\frac{xy}{n}\right) - \left(n + p + \frac{p(1-n^2)}{y}\right)\sinh\left(\frac{xy}{n}\right),$$

$$T_3 := \left(-1 + np - \frac{1-n^2}{y}\right)\cosh\left(\frac{xy}{n}\right) + \left(n - p - \frac{p(1-n^2)}{y}\right)\sinh\left(\frac{xy}{n}\right),$$

$$T_4 := \left(n(1+x) - \frac{n^2}{py} + \frac{(1-n^2)x}{py}\right)\cosh(pxy) + \left(1 - \frac{n}{py} + x - \frac{1-n^2}{(py)^2}\right)\sinh(pxy),$$

$$T_5 := \left(n(1+x) + \frac{n^2}{py} - \frac{(1-n^2)x}{py}\right)\cosh(pxy) - \left(1 + x + \frac{n}{py} - \frac{1-n^2}{(py)^2}\right)\sinh(pxy),$$

$$T_6 := \left(1 + np + \frac{p(1-n^2)}{py}\right)\cosh(pxy) + \left(n + p + \frac{1-n^2}{py}\right)\sinh(pxy),$$

$$T_7 := \left(np - 1 - \frac{p(1-n^2)}{py}\right)\cosh(pxy) + \left(n - p - \frac{1-n^2}{py}\right)\sinh(pxy). \tag{A2}$$

Note that $F(x,y,n,p)$ is continuous at $x=0$.

[1] S. A. Safran, *Statistical Thermodynamics of Surfaces, Interfaces, and Membranes* (Westview, Boulder, 2003).
[2] M. E. Leunissen, A. van Blaaderen, A. D. Hollingsworth, M. T. Sullivan, and P. M. Chaikin, Proc. Natl. Acad. Sci. U.S.A. **104**, 2585 (2007).
[3] M. E. Leunissen, J. Zwanikken, R. van Roij, P. M. Chaikin, and A. van Blaaderen, Phys. Chem. Chem. Phys. **9**, 6405 (2007).
[4] J. Zwanikken and R. van Roij, Phys. Rev. Lett. **99**, 178301 (2007).
[5] M. Bier, J. Zwanikken, and R. van Roij, Phys. Rev. Lett. **101**, 046104 (2008).
[6] J. Zwanikken, J. de Graaf, M. Bier, and R. van Roij, J. Phys.: Condens. Matter **20**, 494238 (2008).
[7] J. de Graaf, J. Zwanikken, M. Bier, A. Baarsma, Y. Oloumi, M. Spelt, and R. van Roij, J. Chem. Phys. **129**, 194701 (2008).
[8] S. Sacanna, W. K. Kegel, and A. P. Philipse, Phys. Rev. Lett. **98**, 158301 (2007).
[9] J. W. Gibbs, *Collected Works* (Dover, New York, 1961), Vol. 2.
[10] R. C. Tolman, J. Chem. Phys. **17**, 333 (1949).
[11] J. G. Kirkwood and F. P. Buff, J. Chem. Phys. **17**, 338 (1949).
[12] M. P. A. Fisher and M. Wortis, Phys. Rev. B **29**, 6252 (1984).
[13] E. M. Blokhuis and D. Bedeaux, Physica A **184**, 42 (1992).
[14] V. Talanquer and D. W. Oxtoby, J. Phys. Chem. **99**, 2865 (1995).
[15] J. Barrett, J. Chem. Phys. **111**, 5938 (1999).
[16] M. Born, Z. Phys. **1**, 45 (1920).
[17] A. Onuki, Phys. Rev. E **73**, 021506 (2006).
[18] A. Onuki, J. Chem. Phys. **128**, 224704 (2008).
[19] A. Onuki, Europhys. Lett. **82**, 58002 (2008).
[20] R. Evans, Adv. Phys. **28**, 143 (1979).
[21] R. Evans, in *Proceedings of the Les Houches Summer School of Theoretical Physics*, edited by J. Charvolin, J. F. Joanny, and J. Zinn-Justin, (North-Holland, Amsterdam, 1989), Vol. 48, p. 1.
[22] R. Evans, in *Inhomogeneous Fluids*, edited by D. Henderson (Dekker, New York, 1991), p. 89.
[23] P.-M. König, R. Roth, and K. R. Mecke, Phys. Rev. Lett. **93**, 160601 (2004).